

# SkinGEN: an Explainable Dermatology Diagnosis-to-Generation Framework with Interactive Vision-Language Models

Bo Lin\*  
Zhejiang University  
Binjiang Institute of Zhejiang  
University  
China  
rainbowlin@zju.edu.cn

Yingjing Xu\*  
Zhejiang University  
China  
poppyxu@zju.edu.cn

Xuanwen Bao  
The First Affiliated Hospital, Zhejiang  
University School of Medicine  
China  
xuanwen.bao@zju.edu.cn

Zhou Zhao†  
Zhejiang University  
Shanghai Institute for Advanced  
Study of Zhejiang University  
China  
zhaozhou@zju.edu.cn

Zuyong Zhang†  
Hangzhou Third People's Hospital  
China  
zzynwk@126.com

Zhouyang Wang†  
Hunan University  
China  
wangzhouy@foxmail.com

Jie Zhang  
Zhejiang Chinese Medical University  
China  
zj19820712@126.com

Shuiguang Deng  
Zhejiang University  
China  
dengsg@zju.edu.cn

Jianwei Yin  
Zhejiang University  
China  
zjuyjw@cs.zju.edu.cn

## ABSTRACT

With the continuous advancement of vision language models (VLMs) technology, remarkable research achievements have emerged in the dermatology field, the fourth most prevalent human disease category. However, despite these advancements, VLM still faces "hallucination" in dermatological diagnosis, and due to the inherent complexity of dermatological conditions, existing tools offer relatively limited support for user comprehension. We propose SkinGEN, a diagnosis-to-generation framework that leverages the stable diffusion (SD) method to generate reference demonstrations from diagnosis results provided by VLM, thereby enhancing the visual explainability for users. Through extensive experiments with Low-Rank Adaptation (LoRA), we identify optimal strategies for skin condition image generation. We conduct a user study with 32 participants evaluating both the system performance and explainability. Results demonstrate that SkinGEN significantly improves users' comprehension of VLM predictions and fosters increased trust in the diagnostic process. This work paves the way for more transparent and user-centric VLM applications in dermatology and beyond.

\*Both authors contributed equally to this work.

†Corresponding author.

Permission to make digital or hard copies of all or part of this work for personal or classroom use is granted without fee provided that copies are not made or distributed for profit or commercial advantage and that copies bear this notice and the full citation on the first page. Copyrights for components of this work owned by others than the author(s) must be honored. Abstracting with credit is permitted. To copy otherwise, or republish, to post on servers or to redistribute to lists, requires prior specific permission and/or a fee. Request permissions from [permissions@acm.org](mailto:permissions@acm.org).

ACM MM, 2024, Melbourne, Australia

© 2024 Copyright held by the owner/author(s). Publication rights licensed to ACM.

ACM ISBN 978-x-xxxx-xxxx-x/YY/MM

<https://doi.org/10.1145/nnnnnnn.nnnnnnn>

## CCS CONCEPTS

• Applied computing → Health care information systems.

## KEYWORDS

VLM, stable diffusion, skin disease, diagnosis, visual explainability

## 1 INTRODUCTION

In recent years, large language models (LLMs) [44, 46, 51, 56] and visual language models (VLMs) [4, 10, 22, 27, 49, 58] has witnessed remarkable and swift advancements. Several excellent VLMs such as miniGPT4 [58], openFlamingo [4], cogVLM [49], otter [22] have shown extraordinary multi-model abilities of vision-language understanding and generation. In the healthcare field, VLMs have the potential to revolutionize the entire healthcare continuum by significantly optimizing and improving disease screening and diagnostic procedures, treatment planning, and post-treatment surveillance and care[5]. These advancements offer a profound opportunity to transform healthcare practices, leading to improved patient outcomes and efficiency in healthcare delivery. Existing medical VLMs, such as MedViLL [31], PubMedCLIP [13], LLaVa-Med [23], Med-Flamingo [32], XrayGPT [45], are tailored for visual question answering and report generation on extensive medical datasets. Adapting VLMs for medical visual question-answering is particularly noteworthy, empowering healthcare professionals to pose queries regarding medical images such as CT scans, MRIs, X-rays, and more [17]. Skin diseases are the fourth most common cause of all human diseases, affecting almost one-third of the world's population [15]. SkinGPT-4 [57], an interactive dermatology diagnostic system trained on a vast repository of skin disease images, totaling 52,929 images encompassing both publicly available and proprietary sources, supplemented by clinical concepts and physicians'

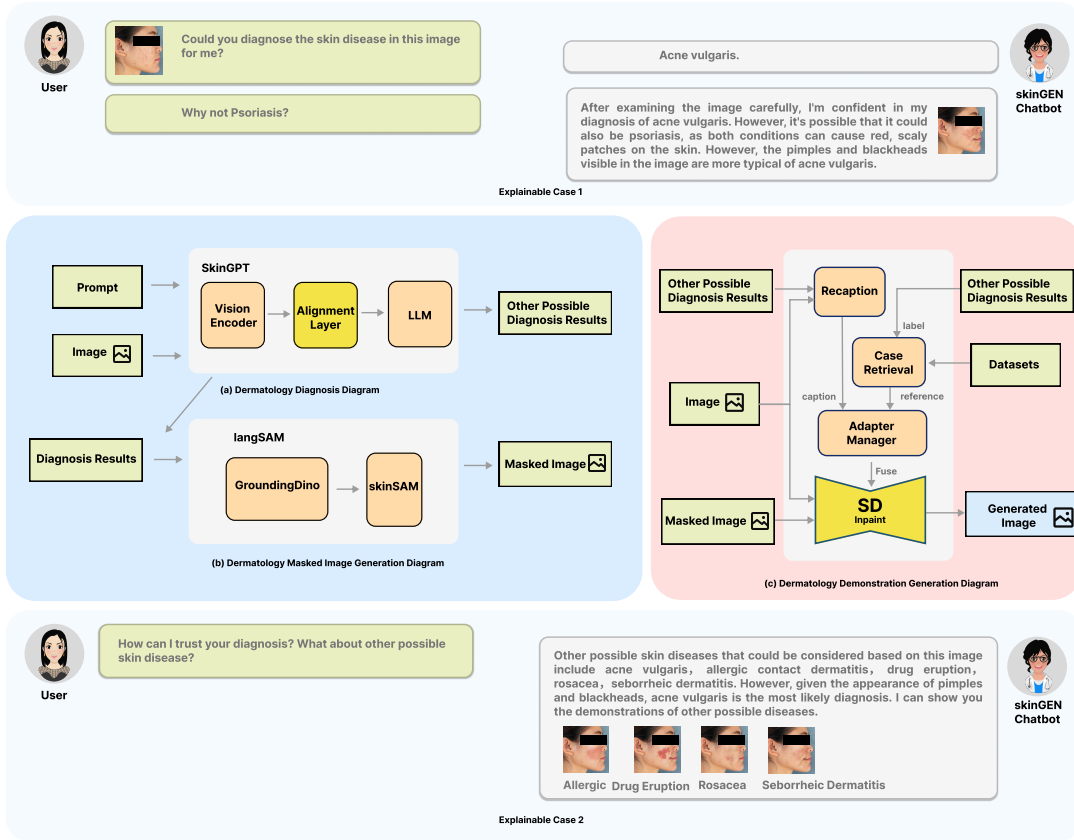


**Figure 1: SkinGEN Explainable Framework: (a) Dermatology Diagnosis Diagram: analyzes the user’s image and provides a diagnosis along with potential alternatives. (b) Dermatology Masked Image Generation Diagram: generate a mask of the affected skin area (c) Dermatology Demonstration Generation Diagram: The Adapter Manager uses LoRA and/or Ip-adapter to generate visual examples of the diagnosed and possible conditions. Case 1: SkinGEN’s diagnosis is questioned by the user. SkinGEN clarifies its reasoning and presents visual examples of similar conditions for comparison. Case 2: The user is unfamiliar with the diagnosis. SkinGEN provides visualizations of similar conditions to facilitate understanding and differentiation.**

notes. Through fine-tuning, the model demonstrated comprehensive efficacy across the diagnostic process.

However, the issue of reliability has increasingly come under scrutiny in these models, particularly in their capacity to deliver accurate and credible information. Frequent occurrences of incorrect or misleading outputs from VLMs, a phenomenon commonly referred to as "hallucination" underscores the paramount importance of ensuring safety in the context of large-scale modeling endeavors [6, 30]. Dermatological conditions may present similar symptoms in their early stages [33], thus complicating accurate diagnosis. The diagnosis of certain dermatological conditions is more challenging compared to other fields, owing to the potential similarity in symptoms and clinical manifestations despite potentially disparate etiologies, which poses significant challenges for patients lacking knowledge about dermatological knowledge. Solely focusing on a model’s predicted diagnosis limits the confidence in the model for clinical decision-making and lacks visual interpretation [38]. It is widely recognized that vision, as an intuitive and easily understandable mode of expression, plays a crucial role in enhancing

user interpretability. This characteristic is particularly critical in the medical domain, where healthcare information often entails high levels of complexity and specialization, necessitating its communication to non-professionals in a manner that is both intuitive and comprehensible to ensure accurate understanding and effective utilization of the information. In this context, the emergence of image generation methods such as SD [37] holds significant importance, offering new possibilities for privacy protection and the generation of illustrative explanations within medical scenarios. Prior work integrating SD [2, 11, 25, 26] with skin-related research primarily focused on expanding datasets for dermatological conditions, without delving into the realm of user interaction.

We introduce SkinGEN, an innovative diagnostic tool designed to enhance the interpretability of VLM through the utilization of the SD method. Users have the capability to upload images depicting dermatological conditions and pose corresponding medical inquiries. SkinGEN, in turn, provides tailored diagnoses or other medical suggestions. In instances where users harbor doubts or encounter confusion regarding the diagnosis, SkinGEN introduces

a feature for demonstrating skin diseases, providing illustrative images depicting alternative dermatological diagnoses similar to the current diagnosis, thereby aiding users in distinguishing between them. Medical information can be transmitted and shared in a more secure and controlled manner through SD, while also enabling the creation of visually intuitive graphical representations. The SkinGEN framework comprises three diagrams: the dermatology diagnosis diagram, the dermatology masked image generation diagram, and the dermatology demonstration generation diagram. By investigating Low-Rank Adaptation (LoRA) within our framework, we established effective techniques for generating realistic and informative skin condition images, improving user comprehension and trust in VLM diagnoses. We recruited 32 participants for our user study. Through comparative experiments, we demonstrate that SkinGEN received positive recognition regarding perceived trust, ease of understanding, and cognitive effort, thereby validating its explainability. Furthermore, in the comprehensive evaluation of the system, participants also provided positive feedback, indicating that the system possessed attributes of being informative, useful, and easy to comprehend. Our contributions are as follows:

- (1) SkinGEN, innovatively uses both interactive VLMs and image generation to improve user understanding and trust. By visualizing the predicted skin condition and other possibilities, SkinGEN makes VLM diagnosis clearer and more reliable for users.
- (2) Through extensive exploration of various training strategies and image synthesis methods, including fine-tuning SD with LoRA and incorporating both text and image prompts, we developed a highly effective solution for generating realistic and informative skin disease images.
- (3) User studies confirm that SkinGEN significantly improves user comprehension and trust in VLM diagnoses. This improvement is achieved by generating personalized visualizations of potential skin conditions directly from user-uploaded images, offering a clear and intuitive understanding of the diagnostic results while preserving user privacy.

## 2 RELATED WORK

### 2.1 Image Generation

Diffusion models, particularly Stable Diffusion(SD) [39], have revolutionized the field of image generation with their ability to synthesize high-quality images aligned with textual prompts. Trained on a massive dataset of images and text descriptions (LAION-5B) [42], SD leverages a latent diffusion process to progressively denoise an initial noise map into the desired image. This process can be further conditioned on various elements, including text prompts, class labels, or low-resolution images, enabling controlled and versatile image generation. The desire for personalized image-generation experiences has driven the exploration of model customization techniques. Fine-tuning SD on domain-specific datasets with designated concept descriptors allows for tailoring the model to specific concepts or styles [21, 41]. This involves minimizing the original loss function of SD on the new data, enabling the model to learn and represent the unique features of the target concepts. LoRA [18] has emerged as a powerful tool for enhancing the efficiency and effectiveness of model customization. By constraining the fine-tuning

process to a low-rank subspace within the original parameter space of SD, LoRA significantly reduces the number of parameters that require updating while preserving the foundational knowledge of the pre-trained model. Building upon the success of text-to-image diffusion models like SD, research has explored efficient and controllable image generation methods, such as Ip-Adapter [54], which leverages the power of both text and image prompts through a decoupled cross-attention mechanism.

### 2.2 Medical VLM

In recent years, significant advancements have been made in the field of LLMs [44, 46, 51, 56] and VLMs [4, 10, 22, 27, 49, 58]. The progress of VLMs has resulted in substantial enhancements in both the quantity and quality of visual instructional data. For instance, MiniGPT4 [58], a generative visual-language model, trained through fine-tuning tasks on specialized datasets, leading to subsequent follow-up endeavors such as PatFig [3], SkinGPT-4 [57], and ArtGPT-4 [55]. These models are designed to address corresponding vision-language tasks across diverse domains. In the medical domain, vision language diagnostic models are regarded as an extremely promising direction for medical advancement, capable of addressing issues related to healthcare resource scarcity and the automation of intelligent diagnosis. Li et al. proposed LLaVa-Med [23], an adaptation of the LLaVa [27], specifically tailored for the medical domain through training on three standard biomedical visual question-answering datasets, which exhibits excellent multimodal conversational capability about a biomedical image. Micheal et al. proposed Med-Flamingo [32], a multimodal few-shot learner that pre-trained on paired and interleaved medical image-text data from publications and textbooks based on OpenFlamingo-9B [4]. These medical VLMs are fine-tuned on generative models using biomedical datasets, allowing the models to assimilate knowledge pertinent to the medical domain, thereby facilitating tasks such as medical diagnostics. The dataset utilized for these medical VLMs is mainly derived from in-vivo diagnostics, such as X-ray and CT scans. Due to the domain gap inherent in a visual model, their diagnostic capabilities for extracorporeal images such as dermatology are relatively limited. Zhou et al. presented SkinGPT-4[57], which is the world's first interactive dermatology diagnostic system powered by an advanced visual language model MiniGPT-4. SkinGPT-4 was trained on an extensive collection of skin disease images (comprising 52,929 publicly available and proprietary images) along with clinical concepts and doctor's notes. The fine-tuned model shows a comprehensive performance in the diagnostic process, user comprehension enhancement, human-centered care, and healthcare equity promotion.

### 2.3 Explainable AI

To satisfy the stringent interpretability requirements of Explainable Artificial Intelligence(XAI), some prior works focus on data explanation so that humans can easily understand them[7, 9, 52, 53]. For example, Chen et al. [9] provided explanatory comments to increase the readability and understandability of the generated code. Wekkeck et al. [52] proposed to explain math theorems by providing detailed derivations. However, these efforts aim to enhance user explainability in specific scenarios by leveraging the language

generation capabilities of large language models. Visual information can enhance user interpretability, and SD possesses powerful visual generation capabilities. Therefore, utilizing the strong visual generation abilities of SD is an important approach to enhancing user interpretability.

Trust, alignment with clinical needs, and ethical deployment are critical components for successfully integrating these models into healthcare workflows [17]. The medical field prioritizes interpretability, while VLM’s inherent lack of interpretability poses significant challenges to healthcare applications. Previous work in dermatoscopic synthetic data generation through SD to mitigate challenges associated with limited labeled datasets, thereby facilitating more effective model training [2, 11, 25, 26]. Akrouf et al. [2] proposed text to image synthesis method for generating high-quality synthetic images of macroscopic skin diseases. Farooq et al. [14] proposed Derm-T2IM that uses natural language text prompts as input and produces high-quality malignant and benign lesion imaging data as the output.

### 3 DERMATOLOGY DEMONSTRATION GENERATION METHOD

#### 3.1 Dataset

This study utilizes two relevant datasets for training the skin disease generation model: Fitzpatrick17k [16] and the recently released SCIN Dataset [50]. Fitzpatrick17k comprises 16,577 clinical images encompassing 114 skin conditions annotated by dermatologists. It also includes discrete labels such as the Fitzpatrick scale, which describes various aspects of skin disease conditions. In contrast, the SCIN Dataset is crowdsourced, collected from 5,000 volunteers, and contains over 10,000 images. SCIN employs a weighted condition labeling system, where a case may be associated with up to 3 skin diseases (conditions). Both datasets exhibit an imbalanced distribution of labels. Fitzpatrick17k’s most frequent condition is psoriasis’ with 653 cases, while the least frequent is pilomatricoma’ with only 52 cases. SCIN demonstrates a similar imbalance. To address this and prepare the data for model training, we sampled three subsets of varying scales: 5-shot, 30-shot, and all. The 5-shot and 30-shot subsets contain random samples across all labels, while the "all" dataset encompasses the entirety of the data. For the training data, we extracted primary skin condition labels and associated features from image-caption pairs, as illustrated in Figure 2. We then employed the Blip2 model [24] to augment the captions with detailed descriptions while also retaining an original dataset with only the extracted labels as captions for comparison purposes.

As Table 1 illustrates, this data preprocessing resulted in 12 subsets (3 scales x 2 datasets x 2 captioning methods), allowing us to investigate the following: (1) **Labeling Method:** We compare the effectiveness of single-label annotations (Fitzpatrick17k) versus multi-weight labels (SCIN). (2) **Scaling Effect:** We analyze the performance across 5-shot, 30-shot, and all datasets to understand the impact of the data scale. (3) **Blip Captioning:** We assess whether the addition of detailed descriptions through Blip2 improves model performance.



Figure 2: Example of an image-caption pair from the training data, where the caption is augmented with a detailed description generated by Blip2 [24].

#### 3.2 Model Training

**Adapter-based Fine-tuning.** To facilitate skin disease image generation conditioned on specific skin conditions, we employed two adapter-based fine-tuning techniques: LoRA [18] and Image Prompt Adapters (Ip-adapter) [54]. Both methods introduce additional trainable layers that integrate seamlessly into the U-Net [40] and Cross-Attention [48] layers of the SD v1.5 [37] image generation pipeline.

**LoRA Configuration.** To investigate the impact of training data volume on model performance, we trained LoRA models using three datasets with varying numbers of samples, as detailed in Table 1. We adjusted the LoRA dimension (dim) according to the dataset size while maintaining consistent hyperparameters across all experiments. These hyperparameters included 20 epochs, a batch size of 2, the AdamW optimizer with 8-bit precision [29], a learning rate of  $1e^{-4}$ , a text encoder learning rate of  $5e^{-5}$ , mixed precision (FP16), and dataset image resolution resized to  $512 \times 512$  pixels.

Table 1: Table of dataset and LoRA parameters

Dataset	Image counts	LoRA dim
f17k-5-shot	570	32
f17k-5-shot-blip		
f17k-30-shot	3470	64
f17k-30-shot-blip		
f17k-All	16576	128
f17k-All-blip		
SCIN-5-shot	1547	32
SCIN-5-shot-blip		
SCIN-30-shot	3341	64
SCIN-30-shot-blip		
SCIN-All	7798	128
SCIN-All-blip		

**Ip-adapter.** Due to limited computational resources, we initially trained LoRA models using all 12 datasets. We conducted experiments to identify the top-performing LoRA model and its corresponding dataset. Subsequently, we trained an Ip-adapter model using the dataset selected from the LoRA training phase. This allowed us to evaluate the skin disease image generation performance of the Ip-adapter model in comparison to the LoRA approach.

### 3.3 LoRA Evaluation

**Quantitative analysis.** The test dataset consists of 100 image-caption pairs sampled from the original training dataset. To evaluate the quality and effectiveness of generated skin disease images, we employed three key metrics to measure the similarity between the original and generated image (using only caption paired with original image): (1) CLIP score [36] for assessing semantical similarity, DINOv2 score [34] for evaluating image structure and quality similarity, and Mean Squared Error (MSE) for measuring pixel-level fidelity. Additionally, we calculated the "blip gain" as the difference in scores between models utilizing blip captions and those without, providing a direct measure of the impact of blip captions on image generation performance. Evaluation metrics presented in Table 2 reveal that the incorporation of blip captions yields only marginal improvements in skin disease image generation. While the Fitzpatrick17k dataset shows a slight average gain of 0.02 in CLIP score and a 0.2 decrease in MSE (indicating better image quality), DINOv2 scores exhibit a decline, suggesting inconsistencies in the benefits across different metrics. Similarly, the SCIN dataset demonstrates a more pronounced average blip gain of 0.09 in CLIP score and a 0.1 reduction in MSE, but DINOv2 scores remain relatively unchanged. Furthermore, analysis of scaling effects reveals no significant positive trends across either dataset. In fact, models trained on the full datasets, particularly within the Fitzpatrick17k set, exhibit a decline in both CLIP and DINOv2 scores compared to the 30-shot models. This suggests potential issues related to data imbalance or overfitting when utilizing the entire dataset, highlighting the need for further investigation and refinement of training strategies to effectively harness the potential of blip captions and larger datasets in this image generation context.

Table 2: Evaluation Metrics for trained LoRA models

Model	CLIP $\uparrow$	DINOv2 $\uparrow$	MSE $\downarrow$
0-shot	0.61	0.69	2.09
f17k_5shot	0.76	0.81	1.31
f17k_5shot_blip	0.77	0.82	1.32
f17k_30shot	0.76	0.82	1.33
f17k_30shot_blip	0.76	0.82	1.31
f17k_all	0.71	0.77	1.25
f17k_all_blip	0.72	0.76	1.25
<b>blip gain</b>	0.02	-0.1	0.2
<b>scaling effect</b>	-0.01	-0.01	-0.25
0-shot	0.63	0.71	2.02
SCIN_5shot	0.71	0.76	1.64
SCIN_5shot_blip	0.75	0.77	1.61
SCIN_30shot	0.74	0.76	1.58
SCIN_30shot_blip	0.76	0.77	1.53
SCIN_all	0.72	0.75	1.62
SCIN_all_blip	0.74	0.76	1.54
<b>blip gain</b>	0.09	0.02	-0.1
<b>scaling effect</b>	0.01	-0.01	-0.01

**Qualitative Analysis of Semantic Understanding.** To further explore the influence of blip captions on the semantic understanding of our trained models, we conducted a qualitative analysis of generated skin disease images. Figure 3 showcases the results of this analysis. We observed that LoRA models trained with longer

training steps (i.e., using larger datasets) exhibited evidence of developing a more nuanced understanding of skin conditions and their presentation. For instance, when generating images using only the label "Psoriasis" as the caption, both the "f17k-30shot-blip" and "fk17k-all-blip" LoRA models produced similar outcomes, depicting psoriasis symptoms on the body. However, when the caption was augmented with the additional description "on her face," the models' behavior diverged. The "f17k-all-blip" LoRA model, trained on the full Fitzpatrick17k dataset, seemingly learned from the data distribution that psoriasis is less likely to occur on the face. Consequently, it generated an image with clear skin on the face, aligning with the typical presentation of the condition. In contrast, the "f17k-30shot-blip" model, trained on a smaller subset of the data, adhered more directly to the provided caption and generated psoriasis symptoms on the girl's face, albeit with a milder appearance. These observations suggest that larger models, exposed to a broader range of examples, develop a more comprehensive understanding of disease characteristics and potential variations, enabling them to generate images that are both realistic and consistent with the provided captions.

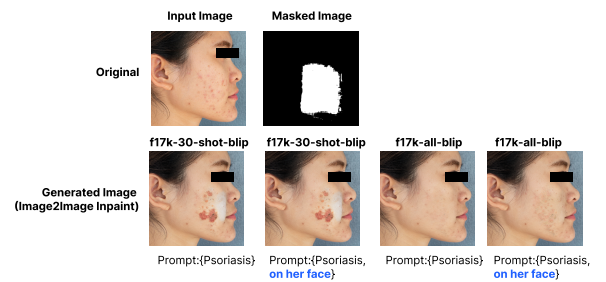


Figure 3: Comparison of skin disease image generation using LoRA models with and without blip captions, showcasing the influence of textual descriptions and training data size on the models' semantic understanding of disease presentation.

**Evaluation of Ip-adapter and Adapter Fusion.** To assess the efficacy of Ip-adapter and the potential benefits of adapter fusion, we designed a comparative experiment with four conditions, as visualized in Figure 4: (1) LoRA (f17k\_30shot\_blip), (2) Ip-adapter (0-shot), (3) Ip-adapter (30-shot) fine-tuned on the f17k\_30shot\_blip dataset for 20,000 steps, and (4) Ip-adapter (30-shot) + LoRA (30-shot) representing adapter fusion. Our findings indicate that the fused adapter configuration (condition 4) yielded the most favorable outcomes, generating disease patterns that closely resembled the reference images. Notably, the 0-shot Ip-adapter demonstrated an inherent ability to grasp the task and synthesize skin disease patterns, albeit with less accuracy compared to the fine-tuned and fused models. Surprisingly, the fine-tuned Ip-adapter (30-shot) produced the least desirable results, suggesting potential challenges related to overfitting or optimization during the fine-tuning process.

## 4 IMPLEMENTATION

### 4.1 Explainable Framework

SkinGEN is a diagnosis assistant in the field of dermatology, which provides a dermatology diagnosis-to-generation solution to increase VLM's visual explainability to users. For skin diseases that

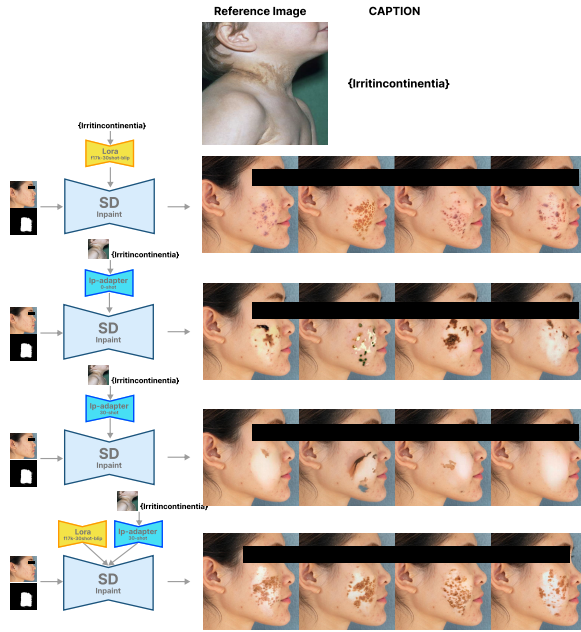


**Figure 4: Comparison of Skin Disease Image Generation using Different Adapter Configurations.** The figure showcases example outputs from four experimental conditions: (1) LoRA model, (2) 0-shot Ip-adapter, (3) fine-tuned Ip-adapter, and (4) fused Ip-adapter and LoRA model. The results highlight the advantages of adapter fusion in generating disease patterns that closely resemble the reference images.

are difficult to distinguish, it utilizes SD to provide visual demonstrations for similar skin diseases to help patients better distinguish between them. As illustrated in Fig. 1, the solution consists of three diagrams: dermatology diagnosis diagram, dermatology masked image generation diagram, and dermatology demonstration generation diagram. In the dermatology diagnosis diagram, we employ SkinGPT-4 to diagnose the uploaded image, obtaining diagnostic outcomes and other potential skin disease results. In the dermatology masked image generation diagram, we first utilize the GroundingDINO model to identify the location of skin disease within the image based on the prompt of skin conditions. Subsequently, the skinSAM model is employed to segment the regions affected by skin diseases, generating a masked image. In the dermatology demonstration generation diagram, Our exploration of adapter methods led to the development of a robust image generation approach. In the subsequent sections, we will delve into the technical details of implementing these three diagrams.

## 4.2 Dermatology Diagnosis

SkinGPT-4 is an interactive system in the field of dermatology designed to provide a natural language-based diagnosis of skin disease images [57]. It was trained on an extensive collection of skin disease images (comprising 52,929 publicly available and proprietary images) along with clinical concepts and doctors' notes. The

architecture of SkinGPT-4 comprises three modules: the visual encoder, the projection layer, and an advanced large language decoder. The visual encoder includes the Vision Transformer(ViT)[12] and Q-Transformer[8], which can encode the input image into image embedding account for the image's context. The function of the alignment layer is to align the semantics of the text space with the semantics of the image space. The SkinGPT-4 utilizes the Vicuna[51] and Llama[46] as the language decoder, which can perform a wide range of complex linguistic tasks.

We utilize SkinGPT-4 to accept dermatology images and questions from users. Upon receiving a query from the user, SkinGPT-4 provides corresponding answers. Fig. 1 shows two examples of SkinGPT-4, it can be observed that SkinGPT-4 possesses knowledge and understanding of dermatological conditions, enabling it to assist patients in making preliminary diagnoses and providing relevant suggestions. Due to the inherent complexity in diagnosing skin diseases, SkinGPT-4 may not always provide entirely accurate diagnostic outcomes; however, it is also capable of generating other possible diagnoses for the given image. The pipeline of skin disease is in Fig. 5. The user uploads an image of skin disease and poses questions, the process by which SkinGPT-4 handles user prompts can be divided into two steps: encoding and decoding. In the process of encoding, the visual encoder extracts vital features and generates an embedding of the image based on the features. The alignment layer synchronizes the visual information and natural language, thus the visual embedding is transformed into an embedding with textual semantics. The input prompt is tokenized by the tokenizer and then it concatenates with the transformed visual embedding. In the processing of decoding, we input the concatenated embedding into Vicuna, which generates the text-based diagnosis. To obtain both the diagnostic result and other possible skin results for the current dermatological image, we designed two tasks as shown in Fig. 5. The first task aims to obtain the diagnostic result of the skin disease in the input image, the prompt designed for the first task is "Could you diagnose the skin disease in this image for me?". We aim to obtain the diagnostic result of a skin disease, such as "acne". The second task aims to identify other possible skin diseases, the prompt designed for the second task is "What's the other possible skin disease in this picture?". We expect to receive a list containing possible skin disease outcomes, for instance, ["Atopic dermatitis", "Hives or urticaria", "Psoriasis", "Contact dermatitis", "Eczema"].

## 4.3 Dermatology Masked Image Generation

To generate masked images of skin disease, we apply the lang-segment-anything(lang-SAM) pipeline. Different from the global segmentation tasks the segment anything model(SAM) [20] provided, the lang-SAM can identify and segment the dermatological area by prompt in the skin image. Fig. 6 illustrates the process of dermatology masked image generation. First, we use the GroundingDino model to identify the skin disease region in the uploaded image. GroundingDINO [28] is an object identification model that requires a prompt input, when the prompt is set to a specific skin disease, the GroundingDINO is capable of returning the bounding box indicating the location of the specific skin disease within the current image. After obtaining the bounding box position of the skin disease, we proceed to generate the mask of this image. We

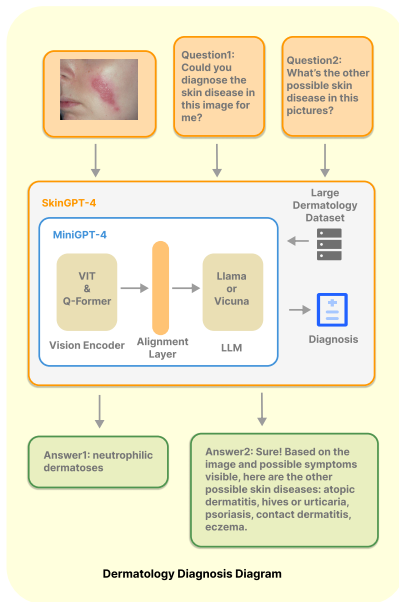


Figure 5: Dermatology Diagnosis with SkinGPT-4 [57].

input the current skin disease image along with the bounding box information into the skinSAM, it subsequently returns a masked image of the skin disease.

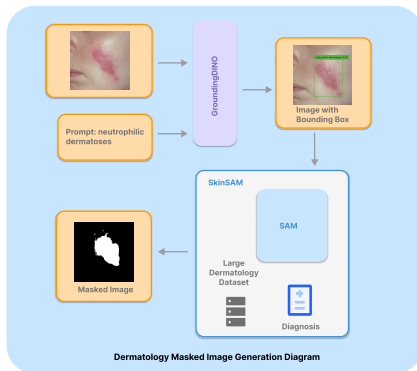


Figure 6: Dermatology masked image generation diagram with object identification and mask generation.

It is noteworthy that the SAM is trained on the SA-1B dataset of 11 million images and 1.1 billion masks, which can understand the visual concepts deeply. To adapt the SAM for skin cancer segmentation tasks better, we employed the skinSAM [19], which is a fine-tuned version of the SAM validated on HAM10000 dataset [47] specifically designed for skin diseases which includes 10015 dermoscopic images. We downloaded the weights of the skinSAM from Huggingface for our use. Figure 6 provides masked image examples generated by lang-SAM.

#### 4.4 Dermatology Image Generation

Building upon the generative model experiments in Section 3, we propose a tailored image generation diagram for dermatology applications, addressing the challenge of generating skin disease images

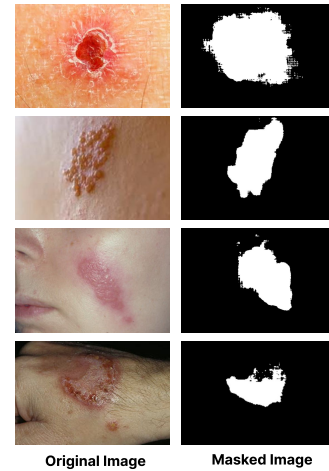


Figure 7: Example of masked images generated by lang-sam from dermatological images.

based on user-provided input. The pipeline comprises three key components: (1) **Recaptioning**: We employ BLIP2 [24] to automatically generate descriptive captions for user-provided images. This step enhances the input information and provides a more informative context for subsequent stages. (2) **Case Retrieval**: A case retrieval module searches for relevant skin disease cases within a curated database based on the input image label and BLIP2-generated caption. This module aims to identify existing cases with similar characteristics to guide the image generation process. (3) **Adapter Manager**: This module dynamically selects the appropriate image generation strategy based on the case retrieval results. If relevant cases are found, we utilize a combination of LoRA and IP-Adapter to leverage both textual and visual information from the retrieved cases. In the absence of similar cases, we employ LoRA with a standard text-to-image generation approach using the BLIP2 caption as input. Figure 8 illustrates the overall architecture of the proposed dermatology image generation pipeline.

## 5 USER STUDY

### 5.1 Experiment Design

To evaluate the effectiveness of different skin disease explanation systems, we conducted an online user study with 32 participants recruited through social media. All participants had agreed to collect data and record the experiment process. The study employed a within-subjects design where each participant interacted with three distinct systems: (1) **System 1 (SkinGPT)**: This system provided plain text explanations of skin conditions generated by the SkinGPT. (2) **System 2 (Reference Case Retrieval)**: This system retrieved and presented visually similar cases from a database of skin disease images along with their corresponding diagnoses. (3) **System 3 (SkinGEN)**: Our proposed SkinGEN system, diagnosed skin conditions based on user-uploaded images and generated personalized visualizations of the identified diseases.

The experiment was implemented using a multi-modal chatbot application built with Gradio [1]. Participants engaged in conversations with the chatbot, providing information about their skin

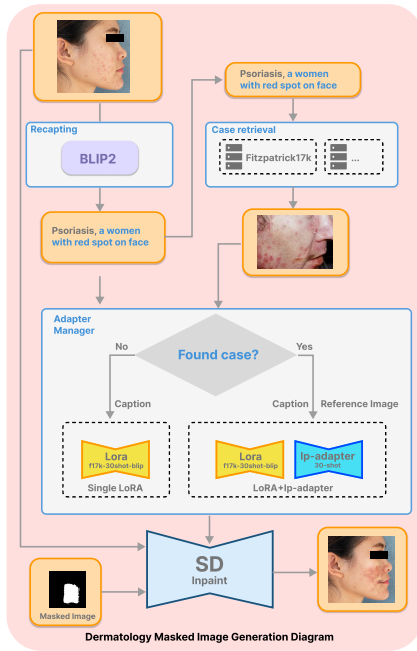


Figure 8: Dermatology image generation diagram with recapturing, case retrieval, and adapter management modules.

concerns and receiving explanations from each system in a randomized order.

## 5.2 Evaluation of Chatbot Explainability

To assess user perceptions of the chatbot system’s explainability, we employed established trust-related metrics inspired by prior work [35, 43]. These metrics focus on evaluating both system and user interface explainability through the lens of user trust. Following interactions with each system, participants completed a questionnaire designed to measure three key constructs: (2) **Perceived Trust**: The extent to which users felt they could rely on the system’s information and recommendations. (2) **Ease of Understanding**: The clarity and comprehensibility of the system’s explanations and conversational flow. (3) **Cognitive Effort**: The mental effort required by users to understand and process the information provided by the system.

All participants engaged in interactions with each of the three chatbot systems in a randomized order. During each system test, participants selected a skin disease image online (restricted to 114 labels within the Fitzpatrick17k dataset) and input it into the SkinGEN user interface to initiate a conversation with the chatbot. After each interaction, users rated their experience based on the questions presented in Table 3.

## 5.3 Result

**Explainability** The user study results, as visualized in Figure 9, provide insights into user perceptions of trust, ease of understanding, and cognitive effort associated with different skin disease explanation systems. System 1, which represents the plain SkinGPT explanation, achieved a moderate level of perceived trust and ease

Table 3: System Explainability Evaluation

Question
Repeated measure (3 conditions)
Perceived Trust: I can trust the system.
Ease of Understanding: The conversation with the system is easy to understand.
Cognitive Effort: I easily found the information I was asking for.
Rated once
SkinGEN’s diagnosis is correct or relevant.
The description provided by SkinGEN is informative.
The suggestions offered by SkinGEN are useful.
I would be willing to use SkinGEN in the future.
The generated skin disease image looks realistic.
I find SkinGEN to be a useful system.

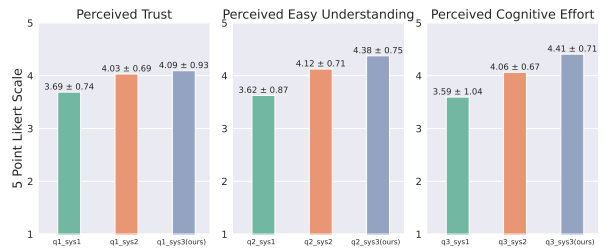


Figure 9: Perceived explainability ratings (Mean ± SD) for the three explanation systems: SkinGPT (sys1), SkinGPT + reference case retrieval (sys2), and SkinGEN (sys3, ours).

of understanding. System 2, based on finding reference cases in a database, showed slightly higher scores in both categories. Notably, System 3 (SkinGEN), our proposed method for diagnosis and skin disease image generation based on user-uploaded images, outperformed both baseline systems across all three metrics. Users perceived SkinGEN explanations as significantly more trustworthy, easier to understand, and requiring less cognitive effort to interpret. This suggests that the ability to generate personalized visualizations of skin conditions based on individual cases resonates with users and enhances their comprehension of the provided information.

**System Performance.** The results of the user questionnaire, summarized in Table 4, demonstrate positive user perceptions of SkinGEN’s performance. Participants generally agreed that SkinGEN’s diagnoses were accurate or relevant (mean = 4.16), the provided descriptions were informative (mean = 4.41), and the suggestions offered were useful (mean = 4.31). Furthermore, users expressed a willingness to utilize SkinGEN in the future (mean = 4.31) and perceived the system as useful overall (mean = 4.38). The visual fidelity of the generated skin disease images also received positive feedback (mean = 4.16), indicating that users found the images to be realistic. These findings suggest that SkinGEN effectively addresses user needs in understanding and visualizing skin conditions, fostering trust and confidence in the system’s capabilities.

## 6 DISCUSSION&CONCLUSION

In this paper, we reveal a shortcoming of previous medical VLM, especially in the dermatology field. the lack of visual explainability



**Table 4: Questionnaire Results: Mean and Standard Deviation**

Question	Mean $\pm$ SD
SkinGEN's diagnosis is correct or relevant.	4.16 $\pm$ 0.63
The description provided by SkinGEN is informative.	4.41 $\pm$ 0.61
The suggestions offered by SkinGEN are useful.	4.31 $\pm$ 0.78
I would be willing to use SkinGEN in the future.	4.31 $\pm$ 0.78
The generated skin disease image looks realistic.	4.16 $\pm$ 0.77
I find SkinGEN to be a useful system.	4.38 $\pm$ 0.75

limits users' comprehension, and present SkinGEN, which integrates the generation capability to give users visual information of potential skin diseases from diagnosis. To the best of our knowledge, this work is the pioneering work to increase visual explainability via interaction with VLMs in the dermatology field. Our exploration of adapter methods led to the development of a robust image generation approach within SkinGEN, contributing to more transparent and user-centric VLM applications in dermatology. We also show that SkinGEN facilitates users in better understanding and applying medical information, thereby enhancing overall user experience and the quality of healthcare services. We believe this work can motivate further studies on solving explainable problems for users. This endeavor sets the groundwork for more transparent and user-centric VLM applications not only in dermatology but also across various other medical domains.

## REFERENCES

- [1] Abubakar Abid, Ali Abdalla, Ali Abid, Dawood Khan, Abdulrahman Alfozan, and James Zou. 2019. Gradio: Hassle-Free Sharing and Testing of ML Models in the Wild. *arXiv:1906.02569* [cs.LG]
- [2] Mohamed Akrouf, Bálint Gyepesi, Péter Holló, Adrienn Poór, Blága Kincsó, Stephen Solis, Katrina Cirone, Jeremy Kawahara, Dekker Slade, Latif Abid, et al. 2023. Diffusion-based data augmentation for skin disease classification: Impact across original medical datasets to fully synthetic images. In *International Conference on Medical Image Computing and Computer-Assisted Intervention*. Springer, 99–109.
- [3] Dana Aubakirova, Kim Gerdes, and Lufei Liu. 2023. PatFig: Generating Short and Long Captions for Patent Figures. In *Proceedings of the IEEE/CVF International Conference on Computer Vision*. 2843–2849.
- [4] Anas Awadalla, Irena Gao, Josh Gardner, Jack Hessel, Yusuf Hanafy, Wanrong Zhu, Kalyani Marathe, Yonatan Bitton, Samir Gadre, Shiori Sagawa, Jenia Jitsev, Simon Kornblith, Pang Wei Koh, Gabriel Ilharco, Mitchell Wortsman, and Ludwig Schmidt. 2023. OpenFlamingo: An Open-Source Framework for Training Large Autoregressive Vision-Language Models. *arXiv:2308.01390* [cs.CV]
- [5] Pierre Baldi. 2021. *Deep learning in science*. Cambridge University Press.
- [6] Rishi Bommasani, Drew A Hudson, Ehsan Adeli, Russ Altman, Simran Arora, Sydney von Arx, Michael S Bernstein, Jeannette Bohg, Antoine Bosselut, Emma Brunskill, et al. 2021. On the opportunities and risks of foundation models. *arXiv preprint arXiv:2108.07258* (2021).
- [7] William Castillo-González, Carlos Oscar Lepez, and Mabel Cecilia Bonardi. 2022. Chat GPT: a promising tool for academic editing. *Data and Metadata* 1 (2022), 23–23.
- [8] Yevgen Chebotar, Quan Vuong, Karol Hausman, Fei Xia, Yao Lu, Alex Irpan, Aviral Kumar, Tianhe Yu, Alexander Herzog, Karl Pertsch, et al. 2023. Q-transformer: Scalable offline reinforcement learning via autoregressive q-functions. In *Conference on Robot Learning*. PMLR, 3909–3928.
- [9] Mark Chen, Jerry Tworek, Heewoo Jun, Qiming Yuan, Henrique Ponde de Oliveira Pinto, Jared Kaplan, Harri Edwards, Yuri Burda, Nicholas Joseph, Greg Brockman, et al. 2021. Evaluating large language models trained on code. *arXiv preprint arXiv:2107.03374* (2021).
- [10] Wenliang Dai, Junnan Li, Dongxu Li, Anthony Meng Huat Tiong, Junqi Zhao, Weisheng Wang, Boyang Li, Pascale Fung, and Steven Hoi. 2023. InstructBLIP: Towards General-purpose Vision-Language Models with Instruction Tuning. *arXiv:2305.06500* [cs.CV]
- [11] Onat Dalmaz, Mahmut Yurt, and Tolga Çukur. 2022. ResViT: residual vision transformers for multimodal medical image synthesis. *IEEE Transactions on Medical Imaging* 41, 10 (2022), 2598–2614.
- [12] Alexey Dosovitskiy, Lucas Beyer, Alexander Kolesnikov, Dirk Weissenborn, Xiuhua Zhai, Thomas Unterthiner, Mostafa Dehghani, Matthias Minderer, Georg Heigold, Sylvain Gelly, et al. 2020. An image is worth 16x16 words: Transformers for image recognition at scale. *arXiv preprint arXiv:2010.11929* (2020).
- [13] Sedigheh Eslami, Christoph Meinel, and Gerard De Melo. 2023. Pubmedclip: How much does clip benefit visual question answering in the medical domain?. In *Findings of the Association for Computational Linguistics: EACL 2023*. 1181–1193.
- [14] Muhammad Ali Farooq, Wang Yao, Michael Schukat, Mark A Little, and Peter Corcoran. 2024. Derm-T2IM: Harnessing Synthetic Skin Lesion Data via Stable Diffusion Models for Enhanced Skin Disease Classification using ViT and CNN. *arXiv preprint arXiv:2401.05159* (2024).
- [15] C Flohr and RJBjod Hay. 2021. Putting the burden of skin diseases on the global map. , 189–190 pages.
- [16] Matthew Groh, Caleb Harris, Luis Soenksen, Felix Lau, Rachel Han, Aerin Kim, Arash Koochek, and Omar Badri. 2021. Evaluating deep neural networks trained on clinical images in dermatology with the fitzpatrick 17k dataset. In *Proceedings of the IEEE/CVF Conference on Computer Vision and Pattern Recognition*. 1820–1828.
- [17] Iryna Hartsock and Ghulam Rasool. 2024. Vision-Language Models for Medical Report Generation and Visual Question Answering: A Review. *arXiv preprint arXiv:2403.02469* (2024).
- [18] Edward J Hu, Yelong Shen, Phillip Wallis, Zeyuan Allen-Zhu, Yuanzhi Li, Shean Wang, Lu Wang, and Weizhu Chen. 2021. Lora: Low-rank adaptation of large language models. *arXiv preprint arXiv:2106.09685* (2021).
- [19] Mingzhe Hu, Yuheng Li, and Xiaofeng Yang. 2023. SkinSAM: Empowering Skin Cancer Segmentation with Segment Anything Model. *arXiv:2304.13973* [cs.CV]
- [20] Alexander Kirillov, Eric Mintun, Nikhila Ravi, Hanzi Mao, Chloe Rolland, Laura Gustafson, Tete Xiao, Spencer Whitehead, Alexander C. Berg, Wan-Yen Lo, Piotr Dollár, and Ross Girshick. 2023. Segment Anything. *arXiv:2304.02643* (2023).
- [21] Nupur Kumari, Bingliang Zhang, Richard Zhang, Eli Shechtman, and Jun-Yan Zhu. 2023. Multi-concept customization of text-to-image diffusion. In *Proceedings of the IEEE/CVF Conference on Computer Vision and Pattern Recognition*. 1931–1941.
- [22] Bo Li, Yuanhan Zhang, Liangyu Chen, Jinghao Wang, Jingkang Yang, and Ziwei Liu. 2023. Otter: A Multi-Modal Model with In-Context Instruction Tuning. *arXiv:2305.03726* [cs.CV]
- [23] Chunyuan Li, Cliff Wong, Sheng Zhang, Naoto Usuyama, Haotian Liu, Jianwei Yang, Tristan Naumann, Hoifung Poon, and Jianfeng Gao. 2024. Llava-med: Training a large language-and-vision assistant for biomedicine in one day. *Advances in Neural Information Processing Systems* 36 (2024).
- [24] Junnan Li, Dongxu Li, Silvio Savarese, and Steven Hoi. 2023. Blip-2: Bootstrapping language-image pre-training with frozen image encoders and large language models. In *International conference on machine learning*. PMLR, 19730–19742.
- [25] Wei Li, Shiping Wen, Kaibo Shi, Yin Yang, and Tingwen Huang. 2022. Neural architecture search with a lightweight transformer for text-to-image synthesis. *IEEE Transactions on Network Science and Engineering* 9, 3 (2022), 1567–1576.
- [26] Jiamin Liang, Xin Yang, Yuhao Huang, Haoming Li, Shuangchi He, Xindi Hu, Zejian Chen, Wufeng Xue, Jun Cheng, and Dong Ni. 2022. Sketch guided and progressive growing GAN for realistic and editable ultrasound image synthesis. *Medical image analysis* 79 (2022), 102461.
- [27] Haotian Liu, Chunyuan Li, Qingyang Wu, and Yong Jae Lee. 2023. Visual Instruction Tuning. *arXiv:2304.08485* [cs.CV]
- [28] Shilong Liu, Zhaoyang Zeng, Tianhe Ren, Feng Li, Hao Zhang, Jie Yang, Chunyuan Li, Jianwei Yang, Hang Su, Jun Zhu, et al. 2023. Grounding dino: Marrying dino with grounded pre-training for open-set object detection. *arXiv preprint arXiv:2303.05499* (2023).
- [29] Ilya Loshchilov and Frank Hutter. 2017. Decoupled weight decay regularization. *arXiv preprint arXiv:1711.05101* (2017).
- [30] Atsuyuki Miyai, Jingkang Yang, Jingyang Zhang, Yifei Ming, Qing Yu, Go Irie, Yixuan Li, Hai Li, Ziwei Liu, and Kiyoharu Aizawa. 2024. Unsolvable Problem Detection: Evaluating Trustworthiness of Vision Language Models. *arXiv preprint arXiv:2403.20331* (2024).
- [31] Jong Hak Moon, Hyungyung Lee, Woncheol Shin, Young-Hak Kim, and Edward Choi. 2022. Multi-modal understanding and generation for medical images and text via vision-language pre-training. *IEEE Journal of Biomedical and Health Informatics* 26, 12 (2022), 6070–6080.
- [32] Michael Moor, Qian Huang, Shirley Wu, Michihiro Yasunaga, Yash Dalmia, Jure Leskovec, Cyril Zakka, Eduardo Pontes Reis, and Pranav Rajpurkar. 2023. Med-flamingo: a multimodal medical few-shot learner. In *Machine Learning for Health (ML4H)*. PMLR, 353–367.
- [33] Annamaria Offidani, Oriana Simonetti, Maria Luisa Bernardini, Ayhan Alpogut, Andreina Cellini, and Guido Bossi. 2002. General practitioners' accuracy in diagnosing skin cancers. *Dermatology* 205, 2 (2002), 127–130.
- [34] Maxime Oquab, Timothée Darcet, Théo Moutakanni, Huy Vo, Marc Szafraniec, Vasil Khalidov, Pierre Fernandez, Daniel Haziza, Francisco Massa, Alaaeldin El-Nouby, et al. 2023. Dinov2: Learning robust visual features without supervision. *arXiv preprint arXiv:2304.07193* (2023).

- [35] Pearl Pu and Li Chen. 2006. Trust building with explanation interfaces. In *Proceedings of the 11th international conference on Intelligent user interfaces*. 93–100.
- [36] Alec Radford, Jong Wook Kim, Chris Hallacy, Aditya Ramesh, Gabriel Goh, Sandhini Agarwal, Girish Sastry, Amanda Askell, Pamela Mishkin, Jack Clark, Gretchen Krueger, and Ilya Sutskever. 2021. Learning Transferable Visual Models From Natural Language Supervision. arXiv:2103.00020 [cs.CV]
- [37] Aditya Ramesh, Prafulla Dhariwal, Alex Nichol, Casey Chu, and Mark Chen. 2022. Hierarchical text-conditional image generation with clip latents. *arXiv preprint arXiv:2204.06125* 1, 2 (2022), 3.
- [38] Adrit Rao and Oliver Aalami. 2023. Towards improving the visual explainability of artificial intelligence in the clinical setting. *BMC Digital Health* 1, 1 (2023), 23.
- [39] Robin Rombach, Andreas Blattmann, Dominik Lorenz, Patrick Esser, and Björn Ommer. 2022. High-Resolution Image Synthesis with Latent Diffusion Models. arXiv:2112.10752 [cs.CV]
- [40] Olaf Ronneberger, Philipp Fischer, and Thomas Brox. 2015. U-net: Convolutional networks for biomedical image segmentation. In *Medical image computing and computer-assisted intervention—MICCAI 2015: 18th international conference, Munich, Germany, October 5–9, 2015, proceedings, part III 18*. Springer, 234–241.
- [41] Nataniel Ruiz, Yuanzhen Li, Varun Jampani, Yael Pritch, Michael Rubinstein, and Kfir Aberman. 2023. Dreambooth: Fine tuning text-to-image diffusion models for subject-driven generation. In *Proceedings of the IEEE/CVF Conference on Computer Vision and Pattern Recognition*. 22500–22510.
- [42] Christoph Schuhmann, Romain Beaumont, Richard Vencu, Cade Gordon, Ross Wightman, Mehdi Cherti, Theo Coombes, Aarush Katta, Clayton Mullis, Mitchell Wortsman, Patrick Schramowski, Srivatsa Kundurthy, Katherine Crowson, Ludwig Schmidt, Robert Kaczmarczyk, and Jenia Jitsev. 2022. LAION-5B: An open large-scale dataset for training next generation image-text models. arXiv:2210.08402 [cs.CV]
- [43] Simone Stumpf, Simonas Skrebe, Graeme Aymer, and Julie Hobson. 2018. Explaining smart heating systems to discourage fiddling with optimized behavior. In *IUI Workshops*.
- [44] Rohan Taori, Ishaan Gulrajani, Tianyi Zhang, Yann Dubois, Xuechen Li, Carlos Guestrin, Percy Liang, and Tatsunori B. Hashimoto. 2023. Stanford Alpaca: An Instruction-following LLaMA model. [https://github.com/tatsu-lab/stanford\\_alpaca](https://github.com/tatsu-lab/stanford_alpaca).
- [45] Omkar Thawkar, Abdelrahman Shaker, Sahal Shaji Mullappilly, Hisham Cholakkal, Rao Muhammad Anwer, Salman Khan, Jorma Laaksonen, and Fahad Shahbaz Khan. 2023. Xraygpt: Chest radiographs summarization using medical vision-language models. *arXiv preprint arXiv:2306.07971* (2023).
- [46] Hugo Touvron, Thibaut Lavril, Gautier Izacard, Xavier Martinet, Marie-Anne Lachaux, Timothée Lacroix, Baptiste Rozière, Naman Goyal, Eric Hambro, Faisal Azhar, Aurelien Rodriguez, Armand Joulin, Edouard Grave, and Guillaume Lample. 2023. LLaMA: Open and Efficient Foundation Language Models. arXiv:2302.13971 [cs.CL]
- [47] Philipp Tschandl, Cliff Rosendahl, and Harald Kittler. 2018. The HAM10000 dataset, a large collection of multi-source dermatoscopic images of common pigmented skin lesions. *Scientific data* 5, 1 (2018), 1–9.
- [48] Ashish Vaswani, Noam Shazeer, Niki Parmar, Jakob Uszkoreit, Llion Jones, Aidan N Gomez, Lukasz Kaiser, and Illia Polosukhin. 2017. Attention is all you need. *Advances in neural information processing systems* 30 (2017).
- [49] Weihang Wang, Qingsong Lv, Wenmeng Yu, Wenyi Hong, Ji Qi, Yan Wang, Junhui Ji, Zhuoyi Yang, Lei Zhao, Xixuan Song, et al. 2023. Cogvlm: Visual expert for pretrained language models. *arXiv preprint arXiv:2311.03079* (2023).
- [50] Abbi Ward, Jimmy Li, Julie Wang, Sriram Lakshminarasimhan, Ashley Carrick, Bilson Campana, Jay Hartford, Pradeep Kumar S, Tiya Tiyasirichokchai, Sunny Virmani, Renee Wong, Yossi Matias, Greg S. Corrado, Dale R. Webster, Dawn Siegel, Steven Lin, Justin Ko, Alan Karthikesalingam, Christopher Semturs, and Pooja Rao. 2024. Crowdsourcing Dermatology Images with Google Search Ads: Creating a Real-World Skin Condition Dataset. arXiv:2402.18545 [cs.CY]
- [51] Jerry Wei, Jason Wei, Yi Tay, Dustin Tran, Albert Webson, Yifeng Lu, Xinyun Chen, Hanxiao Liu, Da Huang, Denny Zhou, and Tengyu Ma. 2023. Larger language models do in-context learning differently. arXiv:2303.03846 [cs.CL]
- [52] Sean Welleck, Jiacheng Liu, Ximing Lu, Hannaneh Hajishirzi, and Yejin Choi. 2022. Naturalprover: Grounded mathematical proof generation with language models. *Advances in Neural Information Processing Systems* 35 (2022), 4913–4927.
- [53] Xuansheng Wu, Haiyan Zhao, Yaochen Zhu, Yucheng Shi, Fan Yang, Tianming Liu, Xiaoming Zhai, Wenlin Yao, Jundong Li, Mengnan Du, et al. 2024. Usable xai: 10 strategies towards exploiting explainability in the llm era. *arXiv preprint arXiv:2403.08946* (2024).
- [54] Hu Ye, Jun Zhang, Sibio Liu, Xiao Han, and Wei Yang. 2023. Ip-adapter: Text compatible image prompt adapter for text-to-image diffusion models. *arXiv preprint arXiv:2308.06721* (2023).
- [55] Zhengqing Yuan, Huiwen Xue, Xinyi Wang, Yongming Liu, Zhuangzhe Zhao, and Kun Wang. 2023. ArtGPT-4: Artistic Vision-Language Understanding with Adapter-enhanced MiniGPT-4. *arXiv preprint arXiv:2305.07490* (2023).
- [56] Lianmin Zheng, Wei-Lin Chiang, Ying Sheng, Siyuan Zhuang, Zhanghao Wu, Yonghao Zhuang, Zi Lin, Zhuohan Li, Dacheng Li, Eric. P Xing, Hao Zhang, Joseph E. Gonzalez, and Ion Stoica. 2023. Judging LLM-as-a-judge with MT-Bench and Chatbot Arena. arXiv:2306.05685 [cs.CL]
- [57] Juexiao Zhou, Xiaonan He, Liyuan Sun, Jiannan Xu, Xiuying Chen, Yuetan Chu, Longxi Zhou, Xingyu Liao, Bin Zhang, and Xin Gao. 2023. SkinGPT-4: an interactive dermatology diagnostic system with visual large language model. (2023).
- [58] Deyao Zhu, Jun Chen, Xiaoqian Shen, Xiang Li, and Mohamed Elhoseiny. 2023. Minigpt-4: Enhancing vision-language understanding with advanced large language models. *arXiv preprint arXiv:2304.10592* (2023).